

High Resolution Laser Melting with Brilliant Radiation

A. Streek, P. Regenfuss, H. Exner

Laserinstitut der Hochschule Mittweida, Mittweida, D-09648

Keywords

Laser micro sintering, metals, additive manufacturing, powder, density

REVIEWED

Abstract

Since the discovery of selective laser sintering/melting, numerous modifications have been made to upgrade or customize this technology for industrial purposes. Laser micro sintering (LMS) is one of those modifications: Powders with particles in the range of a few micrometers are used to obtain products with highly resolved structures. Pulses of a q-switched laser had been considered necessary in order to generate sinter layers from these μm -scaled metal powders. However, despite the high resolution, the process repeatability of LMS and the material property of the products have never been completely satisfactory. Recent technological and theoretical progress and the application of brilliant continuous laser radiation have now allowed for efficient laser melting of μm -scaled metal powders. Thereby, it is remarkable that thin sinter layers are generated with a very high laser power. The resulting product resolution is comparable to the one achieved by the LMS regime with q-switched pulses. From the experimental results the performance and potential of this high resolution laser melting regime is demonstrated and the limits of the applicable parameters are deduced.

Introduction

Laser micro sintering is a modification of selective laser sintering, which is based on repeated cycles of coating and selective densification (sintering) of powders or of pasty materials, with the ends of generating, layer by layer, a three-dimensional body. In accordance with the name, the solidification of a product layer is achieved by scanning a laser beam over the powder surface within the cross-section of the desired object. The material passes through a transitory melt phase. Since its invention by Carl Deckard & colleagues [1] selective laser sintering has been upgraded continuously to meet the requirements for the production of functional components [2]. A considerable contribution to the improvement of resolution was the modification and optimization of the already established technology in 2001 by Laserinstitut der Hochschule Mittweida. It resulted in a technology termed laser micro sintering. The main features are the employment of q-switched laser pulses and the use of powder with particle sizes in the μm -range. Resolutions have been achieved that approximate the focal diameter (25 μm). A great disadvantage was the limited powder bed density of the applied fine grained powders. Therefore, the recoil forces of the expanding plasma generated by the high intensive q-switched pulses were necessary as a powder condensing momentum. Because of limited intensities of commercially available laser sources in the past a technique for laser sintering of fine grained powders with a cw-Laser had never been accomplished. Applying new high power laser sources with highest brilliance coupled with a powder compacting mechanism allows for laser micro sintering with cw-radiation, which is commonly designated "laser melting".

Experimental setup

The overall experimental setup for laser melting is principally comparable to the one for laser micro sintering except for a new condensing powder coater [3] and a polygon scanning device. The powder coater was developed to produce highly accurate and dense powder beds of the employed micro powders (Fig. 1.).

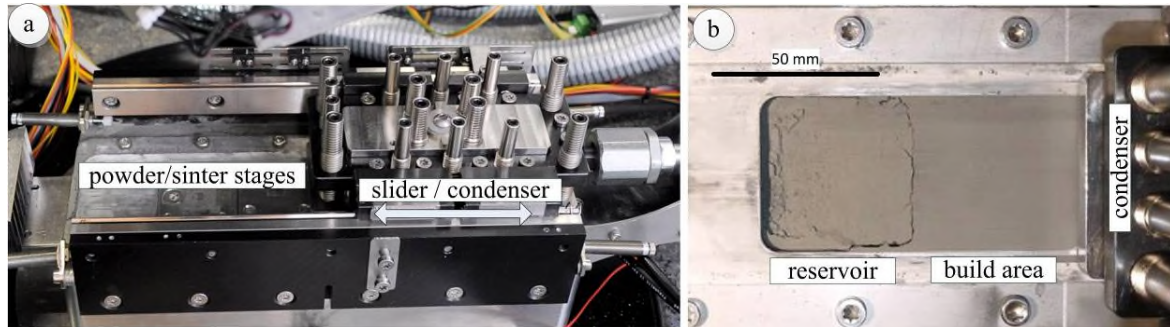


Fig. 1: (a) The novel powder coating forces the powder under high pressure, to flow from the reservoir onto the building platform, to produce highly condensed and homogeneous powder beds of the respective thicknesses. (b) Close view showing the coating properties of the applied molybdenum micro powder.

A YLR-400-LP-AC single-mode fiber laser with a nominal laser power of 400 W from by IPG Laser GmbH (Burbach, Germany) was applied in the continuous wave mode. A 230 mm f-theta-optic, attached to the scanning device, focuses the beam with a gaussian intensity distribution and a radius w_{86} of 35 μm in the plane of the powder bed surface.

For scan velocities up to 10 ms^{-1} a SuperScan-LD-30 from Raylase AG (Weßling, Germany) is used. For fastest beam deflection a 2D polygon mirror with 8 mirror planes combined with a galvanometer operated mirror for lateral beam movement can be used. The polygon scanner is a development of the Laserinstitut der Hochschule Mittweida [4]. Scanning speeds of 10 - 1000 ms^{-1} are achieved with concurrent high precision of 10 μm in a maximum scanfield of 300 x 300 mm and a free aperture of 30 mm.

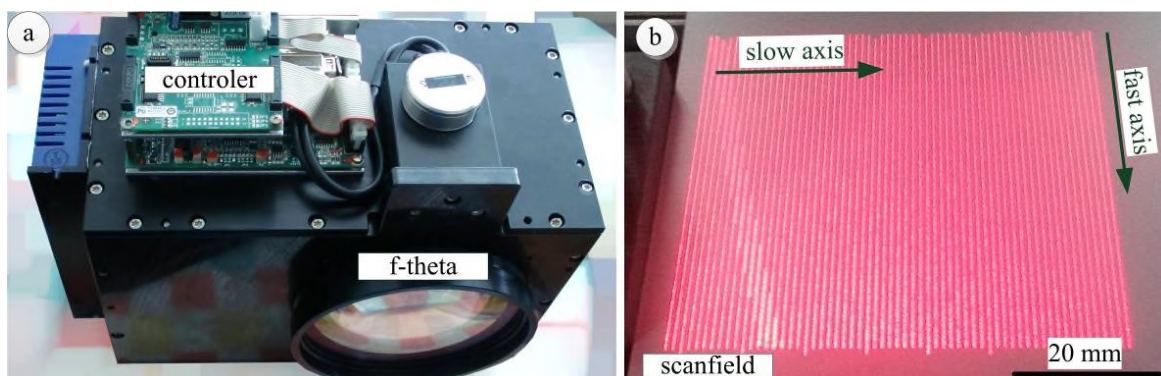


Fig. 2: (a) The 2D - polygon scanning device. Due to the constructional concept it can be easily implemented in any setup as a galvanometer scanner replacement. (b) Scanfield visualized above the building platform by the pilot laser.

The applied powder for the experiments was molybdenum Mo3-7 from Alfa Aesar GmbH & Co KG (Karlsruhe, Germany) (Fig. 3).

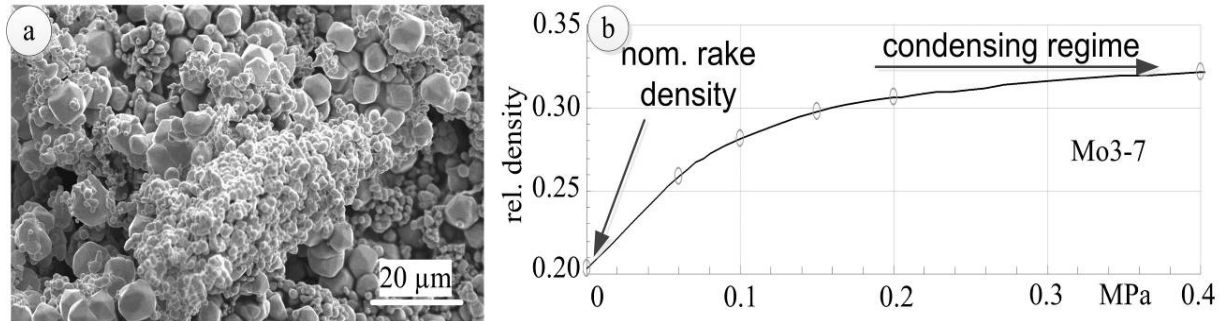


Fig. 3: The applied molybdenum powder Mo3-7. (a) SEM-view of the powder material. As denoted, the grain distributions by mass are $d_{10} = 3 \mu\text{m}$ and $d_{90} = 7 \mu\text{m}$. Therefore the largest number of grains belongs to the fraction of smaller particles and is partially agglomerated. (b) The nominal powder density and therefore the coating density obtained with a classical additive manufacturing setup is 20 %. With the novel powder coating device a compaction of the powder above a density of 30 % is possible.

Background

In a stable laser melting process, the applied process parameters have to allow for a minimum melt depth in the order of the thickness of the coated powder layer and furthermore for effective wetting of the underlying sinter layer. Therefore, the absorbed energy per volume has to suffice for the fusion of the material, which includes the heating to melting point T_M (and above) and the latent heat for the phase transition. However, the absorbed energy has to be lower than the amount, at which the overall ablation, including the expulsion of already molten material, exceeds the material mass added to the site by each powder coating cycle. As already known from investigations of laser micro sintering by high intensive q-switched pulses [5], this will not necessarily lead to a breakdown of the building process but certainly to a noticeable increase of the “height defect” and to deterioration of the micro part resolution.

The resulting melt depth ℓ_m of a massive material (infinite rod) can be transformed to the simple Eq. 1 by the solution of Fourier’s equation for one-dimensional heat conduction, under consideration of the thermal diffusion length ℓ_D , the room temperature T_R and an exponential increasing thermal heat gradient within the material, resulting from a steady increase in surface temperature T_S by the absorbed laser radiation as suggested in [6] and further analyzed in [5].

$$\ell_m = \ln \left(\frac{(T_S - T_R)}{(T_M - T_R)} \right) \cdot \ell_D \quad | T_S > T_M \quad (1)$$

The maximum surface temperature T_S is reached when it equals the boiling point T_B . This limitation defines the highest intrinsic energy that the material can bear without boiling and thus the maximum irradiation time as well as the corresponding intensity. For various materials the dependence of the maximum melt depth on the irradiation time is shown in Fig. 4.

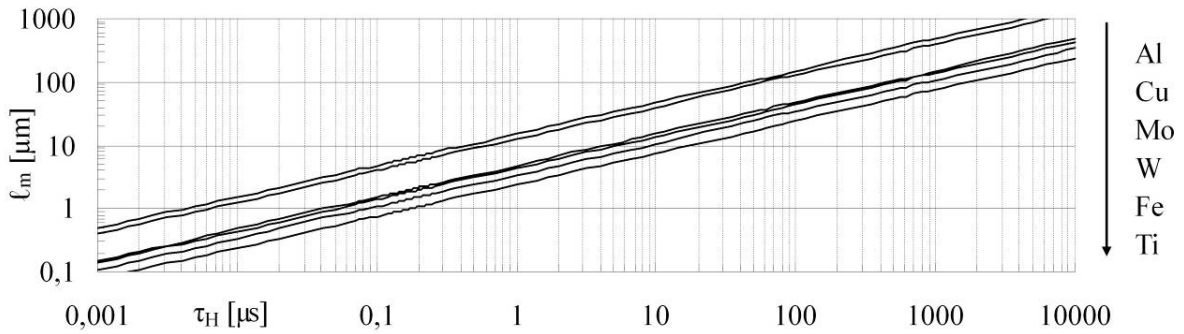
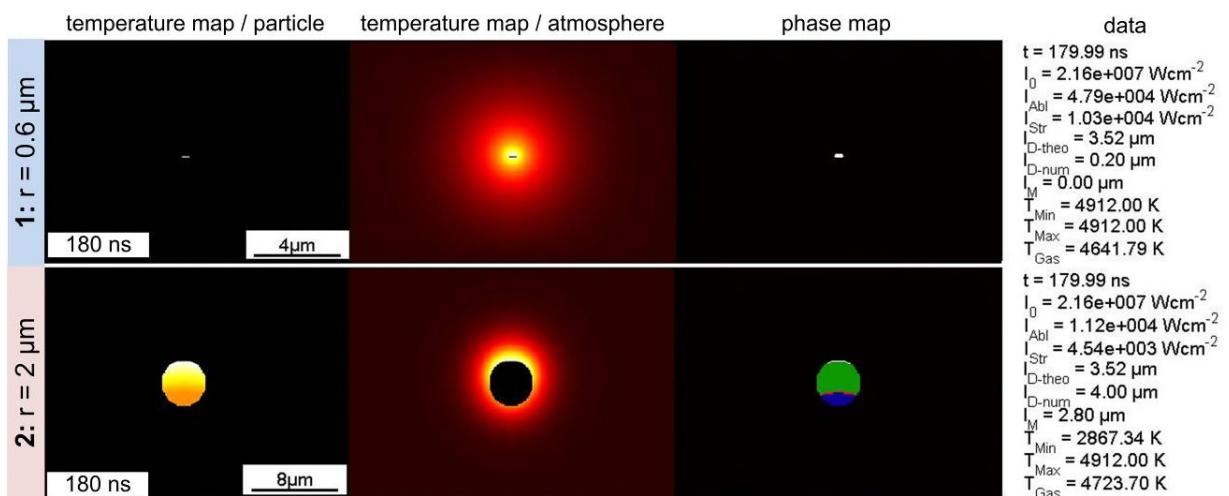


Fig. 4: Achievable melt depths ℓ_m , of different massive metals at irradiation times up to 1 ms under the condition that the material specific boiling temperature is reached at the end of the irradiation. The column on the right lists the elements in the order of their melt depths.

For the investigated molybdenum, under ideal conditions an irradiation time of 50 ns is necessary to achieve a 1 μm depth of the melt pool. The (logarithmically) scaled diagram shows a steady increase of the achievable melt depth along with the irradiation time. Following these simplified estimations, after 500 μs , which means a maximum scan velocity of 0.1 ms^{-1} for a focused 50 μm laser beam, 100 μm melt depth could be achieved. By applying larger focus diameters increased scan velocities can be chosen to achieve the necessary melt depth, but logically the resolution will deteriorate.

As already originally discussed, in [7], overall energy absorption within and energy distribution throughout the powder bed is more complex than the above formulated approximation. Another shortcoming, especially with small powders, is that most often the thermal diffusion length surpasses the particle diameter. In that case, the calculation based on the assumption of an infinite rod will yield an incorrect melt depth.

This fact is principally demonstrated by a numerical temperature field calculation for three laser irradiated powder particles with different radius r [5] with consideration of material expulsion by vaporization and of the latent heats. $I_0 = 2.17 \text{ Wcm}^{-2}$ (Fig. 5: data) is the minimum required intensity to achieve the boiling temperature at the surface of an infinite rod after 180 ns.



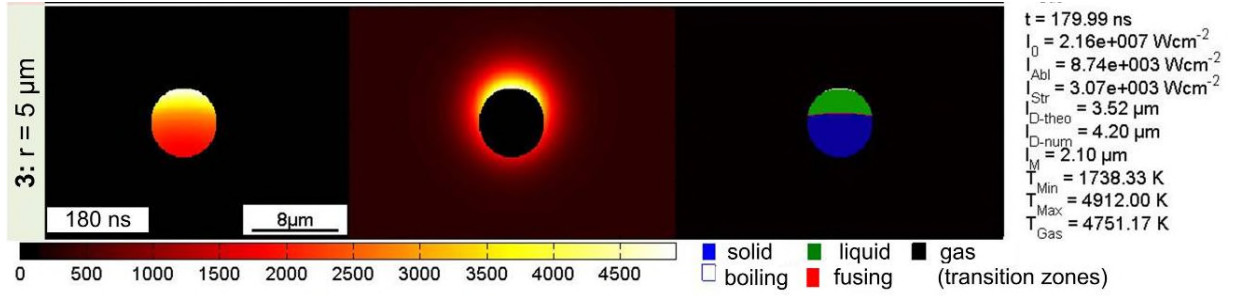


Fig. 5: Temperature field calculation for small molybdenum particles with different sizes. The temperature distributions in the non-volatile particle masses are shown in the left column (temperature map of the particle). The right graphic column (phase map) shows the extent of the phases. The thermal diffusion length $l_{\text{D-theo}}$ (data column) is for particle 1: larger, particle 2: in order of and particle 3: smaller than the particle dimensions.

Data column: The thermal diffusion length $l_{\text{D-theo}}$ is either larger (particle 1) in the same order (particle 2) or smaller (particle 3) compared to the particle dimension. The resulting melt depth l_M increases with decreasing particle diameter.

Boiling and loss of material occurs in the smallest particle (1: $r = 0.6 \mu\text{m}$) due to virtually-zero heat dissipation. Later on, in Fig. 8, these calculated cases 1-3 will be represented with likewise numeration as green circular dots.

The increase of the melt depth in particles with dimensions smaller than the thermal diffusion length is obvious. Therefore, smaller particles should allow for laser melting with higher scan velocities at smaller focus diameters.

Furthermore, due to lack of heat dissipation into deeper layers, thorough melting of the particle can be achieved after the laser irradiation, if the overall transferred energy during the irradiation time is larger than the thermal energy, required to raise the temperature to the boiling point plus the necessary amount of latent heat for the melting of the entire particle mass (or of the residual mass, in case of loss through boiling). For a finite rod this critical depth $d_{\ell m}$ for thorough melting is analytically described in [5] resulting in Eq. 2,

$$d_{\ell m} = \frac{T_B - T_R}{\left(T_M - T_R + \frac{\Delta H_m}{c_p} \cdot \left(1 - \frac{\ell_m}{d_{\ell m}} \right) \right) \left(1 + e^{-2 \frac{d_{\ell m}}{\ell_D}} \right)} \cdot \frac{\sqrt{\pi}}{2} \cdot \sqrt{\frac{\lambda_{th}}{\rho \cdot c_p} \cdot \tau_H} \quad (2)$$

with ΔH_m the specific latent heat of fusion, c_p the specific heat capacity, λ_{th} the thermal conductivity, and ρ the specific density. This critical depth is the maximum depth of thorough melting if the boiling temperature is reached at the end of the irradiation time. For any other final surface temperature T_B has to be substituted by T_S (maximum surface temperature).

In Fig. 6 the maximum critical depths are presented for different materials and irradiation times.

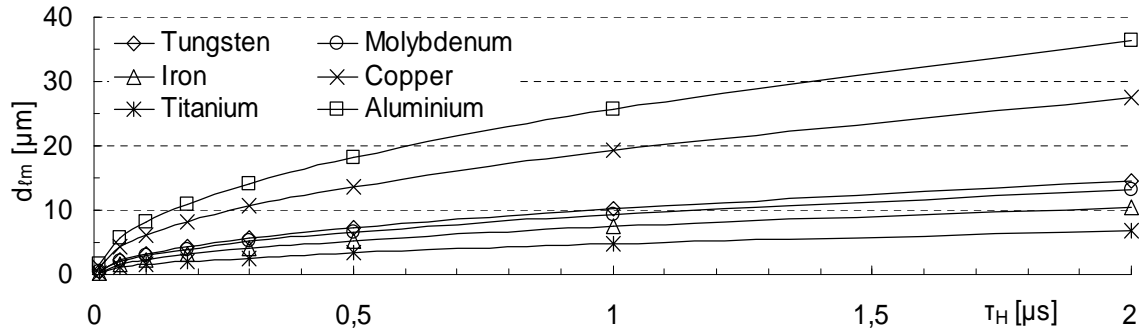


Fig. 6: Critical depths for thorough melting of a finite rod after a certain irradiation time. Due to the large heat conductivity of aluminum and copper these materials also show the deepest thorough melting after short-time laser irradiation. In tungsten and molybdenum a larger amount of energy is storable. Therefore these elements range above iron and titanium with the smallest heat conductivity. 300 K was chosen as environmental temperature T_R in the calculation.

For molybdenum this means that with 1 μs irradiation (velocity $\sim 50 \text{ ms}^{-1}$ @ about 50 μm spot size) the maximum achievable melt depth beneath the surface is almost doubled from 5 μm in bulk material to 10 μm in an isolated particle.

As already mentioned, to achieve the maximum melt depths a specific amount of energy, respectively a specific intensity of the laser, is necessary to just reach the boiling temperature at the end of a chosen irradiation time, at which, with this optimum intensity I_{opt} , the maximum energy storability is reached. Under the same assumptions as for Eq. 1, for a bulk material (infinite rod) the optimal intensity can be analytically described by Eq. 3,

$$I_{opt} = \frac{\lambda_{th}}{\ell_D} \cdot \left(T_B - T_R + \ln \frac{T_S - T_R}{T_M - T_R} \cdot \frac{\Delta H_m}{c_P} \right) \Rightarrow I_{opt} \propto \frac{1}{\sqrt{\tau_H}} \quad (3)$$

which clearly shows the inversely proportional relation between the applicable intensity and the irradiation time τ_H (included in ℓ_D).

Additionally, an intensity window can be defined for laser melting, between a minimum intensity at which the surface temperature just reaches the melt temperature, and a maximum intensity at which an additional amount of latent heat for boiling to the depth of ℓ_m is inserted and most of the material vaporizes. This intensity window (between the dashed lines) and the optimum intensity for different materials are presented in Fig. 7.

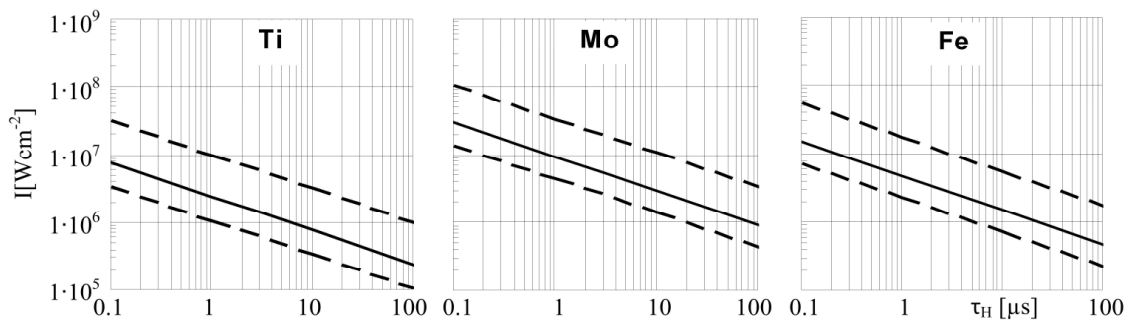


Fig 7: Dependence of the optimal intensity (solid line) and the boundary intensities for different metals on the irradiation time up to 100 μs . The plotted intensities represent the absorbed intensities; the specific absorbance has to be considered for each material.

For the definition of a process window for particles that are considered finite rods, two dependencies have to be observed: Firstly the intensities that lead to a certain temperature after thermal equilibration of the particles with various diameters. These dependencies are linear. Secondly the intensities that effect a certain temperature on the surface of the particles with various diameters at the end of the irradiation time. These dependencies have a curved progression. In Fig. 8 both types of dependencies are displayed for three equilibrium temperatures and for three surface temperatures respectively.

The straight lines in Fig. 8 consist of the intensities by which, disregarding possible over-heating, the cross section of the respective particle absorbs, during the pulse of 180 ns, respective characteristic amounts “min(Q)”, “opt(Q)”, and “max(Q)”. “min(Q)” of energy. “min(Q)” would be just sufficient to convert the entire particle into liquid phase. “opt(Q)” displays the intensities, at which the enthalpy of fusion and additionally the energy that is required to raise the particle temperature to the boiling point is absorbed. This is the intensity at which the entire particle can be converted into a melt phase with boiling temperature. “max(Q)” is the respective minimum energy that is needed to raise the temperature of the entire particle mass to the boiling point, plus the energy for comprehensive evaporation of the particle.

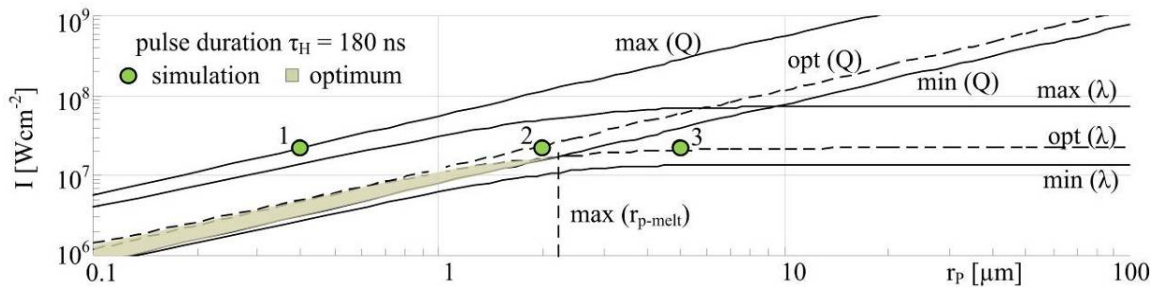


Fig. 8: Characteristic (absorbed) intensities for the fusion of molybdenum particles with a 180 ns laser pulse vs. particle radius. The straight lines are the intensities that yield per pulse the respective net amounts of energies per particle cross section, that would be sufficient to fuse the particle (min(Q)), to fuse and heat the particle to boiling temperature (opt(Q)), and to heat the particle to boiling temperature and evaporate the entire mass (max(Q)) in an imaginary, slow heating process. The bent curves consist of the intensities absorbed from a 180 ns laser pulse that lead to the fusion temperature on the irradiated particle surface (min(λ)), the boiling temperature on the irradiated particle surface (opt(λ)), and to comprehensive boiling of the fused portion of the particle when the irradiated surface has reached the boiling temperature (max(λ)). The green dots represent the chosen parameters of the thermal simulation in Fig. 5.

The second prerequisite is determined by heat conduction of a finite rod described in [8]. As a first approximation the heat conduction in spheric particles has been equated with the one in cylindrical rods of the same cross-section and volume; on the abscissa, the radii of the spheric particles are indicated. The three intensity curves in Fig. 8, max(λ),opt(λ), and min(λ), represent the following thermal conditions at the end of the pulse:

Curve “min(λ)” consists of the intensities at which the particle surfaces have reached the melt temperature at the end of the pulse. Any further energy would lead to the onset of melting in the surface zone. It is considered the minimum energy where partial fusion of particles might be observed. “opt(λ)” are the intensities at which the irradiated surface acquires boiling temperature. With these intensities, the maximum energy can be absorbed by the respective particles without any ablative loss.

With intensities of curve “max(λ)” not only the irradiated surface reaches boiling temperature, but additional energy has also been absorbed that is equivalent to the evaporation enthalpy for the already fused portion of the particle mass. This would imply ablation of the entire liquid phase and preclude any inter-particle fusion.

The shaded section between the curves “min(Q)” and “opt(λ)” denotes the range of particles that can be comprehensively converted into liquid phase without ablation by a 180 ns pulse with the respective intensity.

The largest molybdenum particle (max(r_{p-melt}) in Fig. 8) that can be comprehensively fused has a radius of around 2.1 μm . Larger particles require longer irradiation times (Fig. 9).

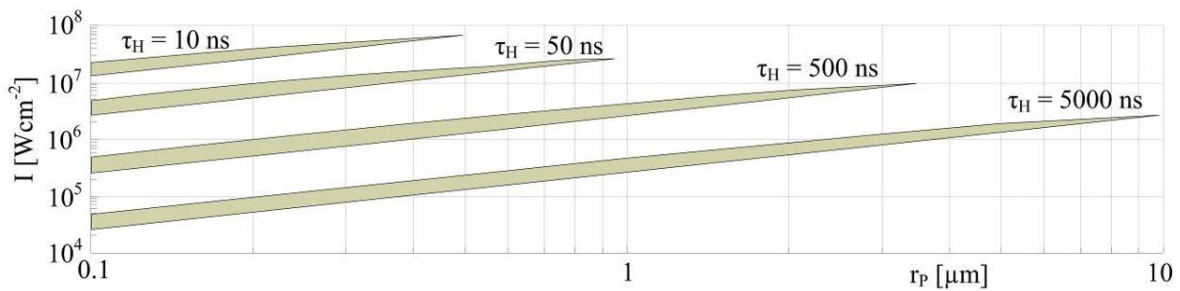


Fig. 9: Intensity/particle-size windows for comprehensive melting of molybdenum particles with laser pulses of various pulse widths, deducted analogue to the values in Fig. 8.

Experimental

For laser micro sintering with q-switched pulses the maximum achievable scan velocity was defined by the given pulse repetition of the laser. For highly dense micro parts the maximum pulse distance (at a beam diameter of 30 μm) was about 10 μm , resulting in scan velocities below 1 ms^{-1} for the applied 20 W q-switched laser with a repetition rate of 80 kHz. The necessary absorbed average intensity for the applied molybdenum powder was about $2 \cdot 10^7 \text{ Wcm}^{-2}$ for 180 ns irradiation time, assuming a material absorbance of $A_{\text{mat}} = 0.30$ from the fresnell equations (Fig. 10).

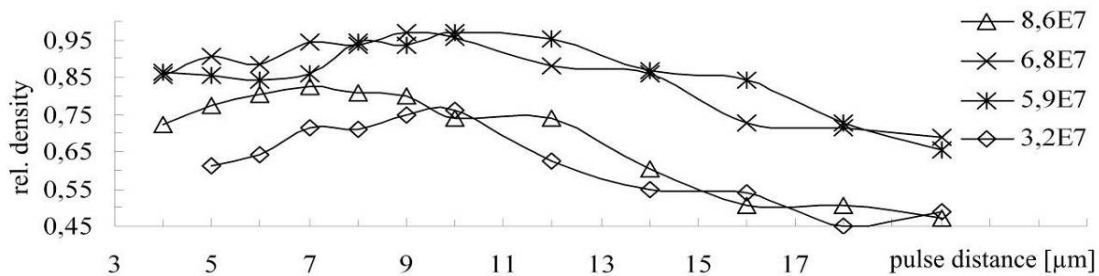


Fig. 10: Resulting sinter densities from molybdenum at various pulse distances and intensities [Wcm^{-2}]. The highest densities are achievable at 5 – 6 Wcm^{-2} (irradiating intensities) and at a pulse overlap of 2-3.

Under consideration of the necessary pulse overlap, the energies for high density micro parts are 2-3 times higher than theoretically estimated (at 2 Wcm^{-2} only one single pulse should suffice to thoroughly melt the particle). Significant increase of the density at higher pulse overlap (at pulse distances around 10 μm) could only be observed if the pulses were set in a continuous sequential

alignment (Fig. 11). Otherwise the densities were almost equal to those achieved with high pulse distances. The remanent heat from the previous pulse seems to support the wetting of the melt. With a cw laser this behavior could also be expected at lower scan velocities that allow for sufficient accumulation of heat.

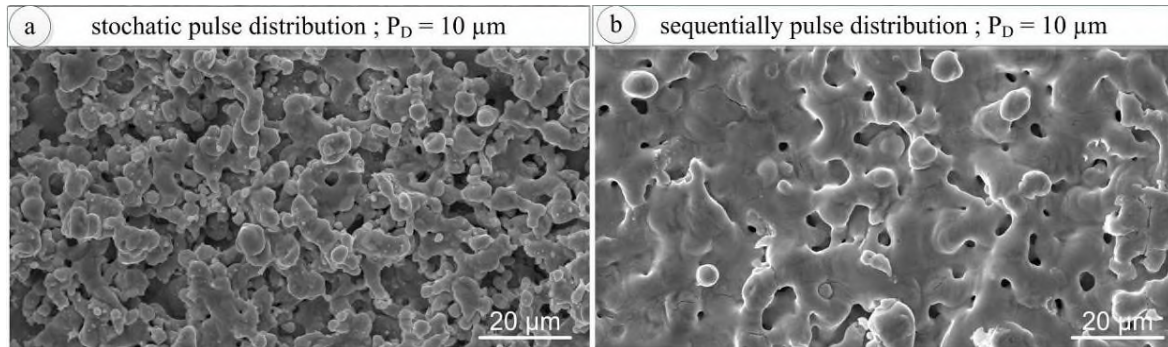


Fig. 11: Sinter structures resulting from (a) stochastic and (b) sequentially line wise pulse positioning. The density of the applied pulses is the same for both specimens. The resulting sinter density was (a) 66 % and (b) 97 %. Sinter parameters: $I_{Av} = 6.5 \cdot 10^7 \text{ Wcm}^{-2}$, $w_0 = 12,5 \mu\text{m}$, $\tau_H = 180 \text{ ns}$, $f_P = 80 \text{ kHz}$, Molybdenum.

Based on the theory, irradiation times of $2.4 \mu\text{s}$ for isolated particles and around $10 \mu\text{s}$ for bulk material should be sufficient/necessary to melt a $10 \mu\text{m}$ sinter layer, if an absorbed intensity between $0.3 \cdot 10^6 \text{ Wcm}^{-2}$ and $0.62 \cdot 10^6 \text{ Wcm}^{-2}$ can be reached. With the 400 W cw laser a maximum intensity of $4 \cdot 10^7 \text{ Wcm}^{-2}$, respectively an absorbed intensity of $1.2 \cdot 10^7 \text{ Wcm}^{-2}$ by the molybdenum powder is achievable at $35 \mu\text{m}$ spot size.

With the attached galvanometer scanner a maximum scan velocity of 8 ms^{-1} , respectively a minimum irradiation time of $4.4 \mu\text{s}$ could be achieved resulting in the sinter densities presented in Fig. 12.

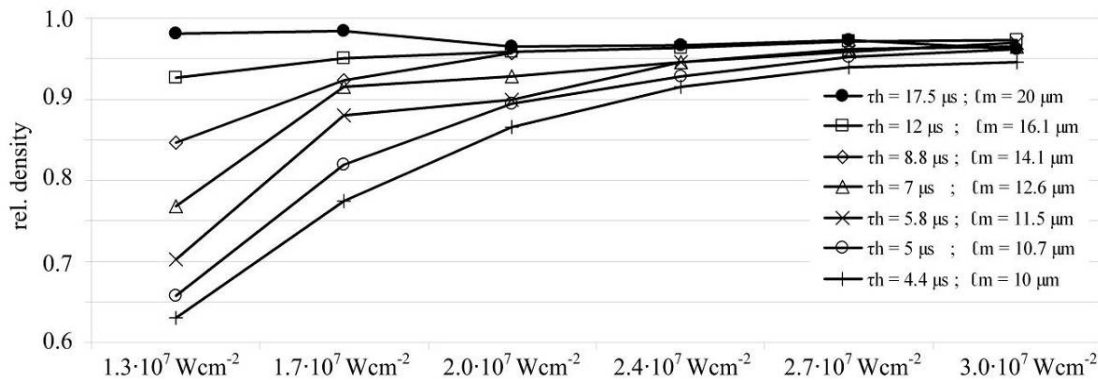


Fig. 12: Resulting sinter densities at various intensities for seven irradiation times corresponding to scan velocities from $2 - 8 \text{ ms}^{-1}$. For comparison, the maximum achievable melt depths l_m calculated with equation 1 are listed.

With a (too) long irradiation time of $17.5 \mu\text{s}$ high sinter densities can be achieved throughout the entire time range. At short irradiation times (respectively with melt depths that will not considerably reach beyond an isolated particle) the resulting density decreases significantly. However, the determined sinter densities in Fig. 12 do not reflect the achieved accuracy of the

specimens. At high intensities and long irradiation times the accuracy of the sintered micro parts deteriorates significantly (Fig. 13: top). The specimens obtained with low intensities and short irradiation times had a porous consistency. Loss of accuracy may be due to poorer fusion of the material in the peripheral zones (Fig. 13: bottom).

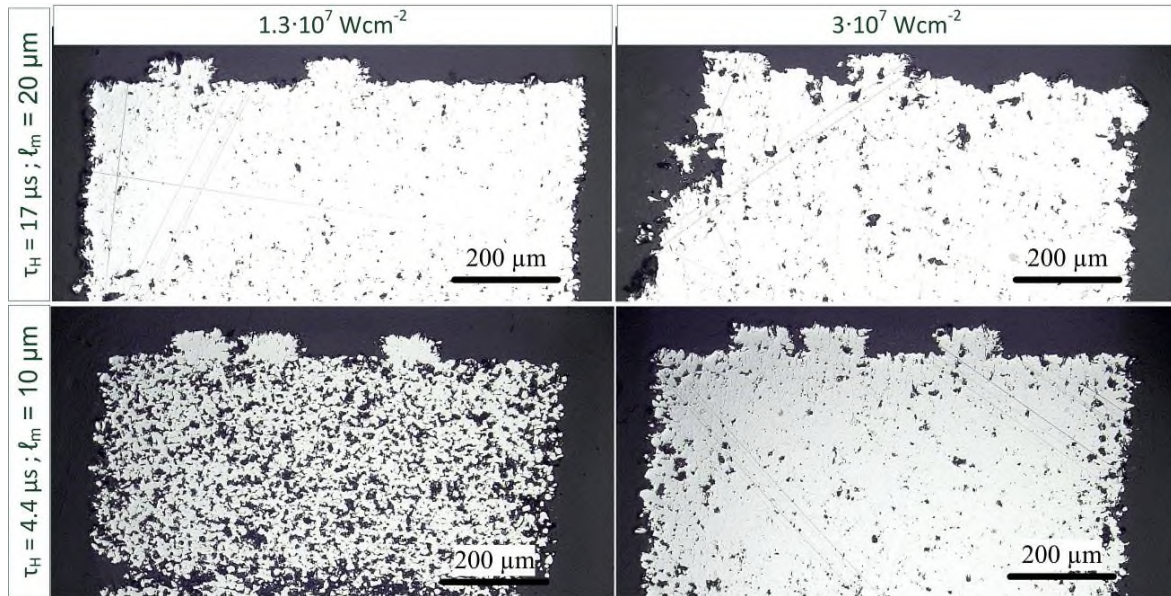


Fig. 13: Cross section preparations of specimens generated at various intensities and irradiation times by a cw laser. Top: 2ms^{-1} ($17.5\ \mu\text{s}$). Bottom: 8ms^{-1} ($4.4\ \mu\text{s}$).

Furthermore, the specimens generated with short irradiation times and low intensities (Fig. 13) showed a behavior of sintering that is familiar from the stochastic pulse distribution (Fig. 11(a)). As expected, specimens with these parameter sets are generated with a noticeably insufficient wetting of the underlying (previously generated) sinter layer. At ideal irradiation times and intensities well defined micro structures at high densities could be generated (Fig. 14).

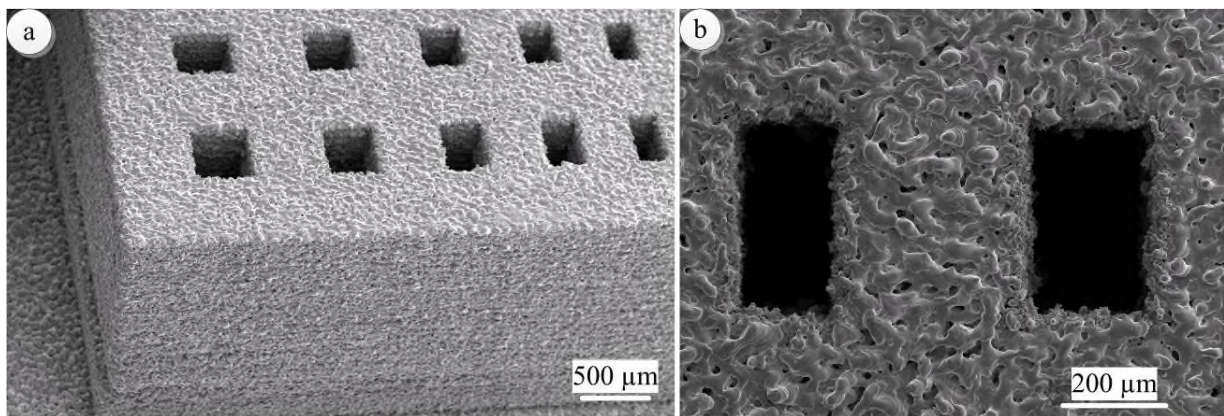


Fig. 14: Surface structures of a laser melted grid. Compared to laser micro sintering relatively thick sinter layers of $10\ \mu\text{m}$ with could be generated with high resolution. This accelerates the building rate significantly compared to the laser micro sintering with merely $1\ \mu\text{m}$ sinter layer.

The resulting roughness of the micro structures was about $35\ \mu\text{m}$ with a final accuracy of about $60\ \mu\text{m}$ for free standing walls (Fig. 15).

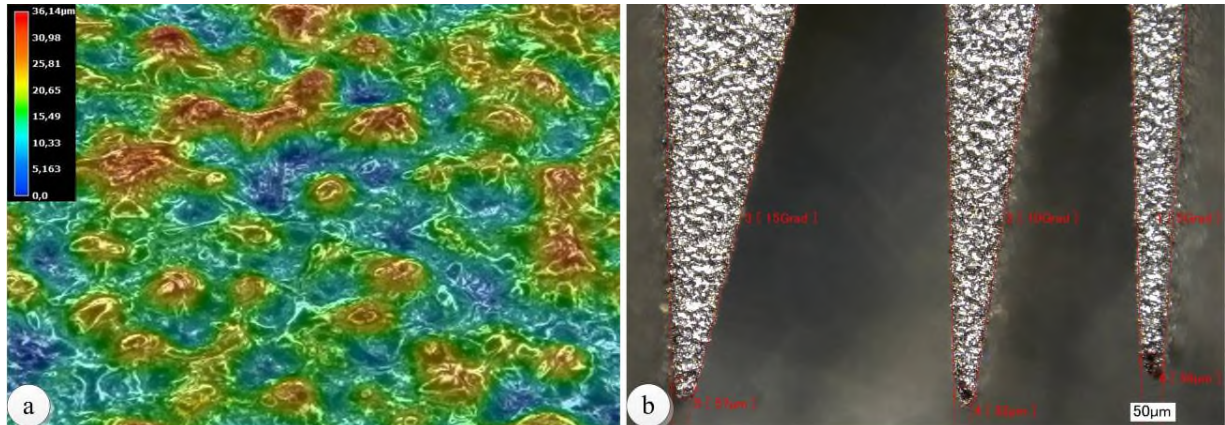


Fig. 15: (a) Surface morphology of the laser melted specimens. (b) Free standing walls with different angles.

With higher scan velocities above 15 ms^{-1} that can be achieved with the polygon scanner device no laser melting of 10 μm thick sinter layers was possible at all. Although theoretically, the critical melt depth for isolated particles at the corresponding irradiation time of about 1 μs should be sufficient (Fig. 6), the melt will never wet the underlying sinter layer.

Upon considerable reduction of the sinter layer thickness down to 1 μm , which is less than the achievable melt depth for the bulk material (Fig. 4), the first solid results could be observed (Fig. 16). This proves the feasibility of laser melting with high scan velocities.

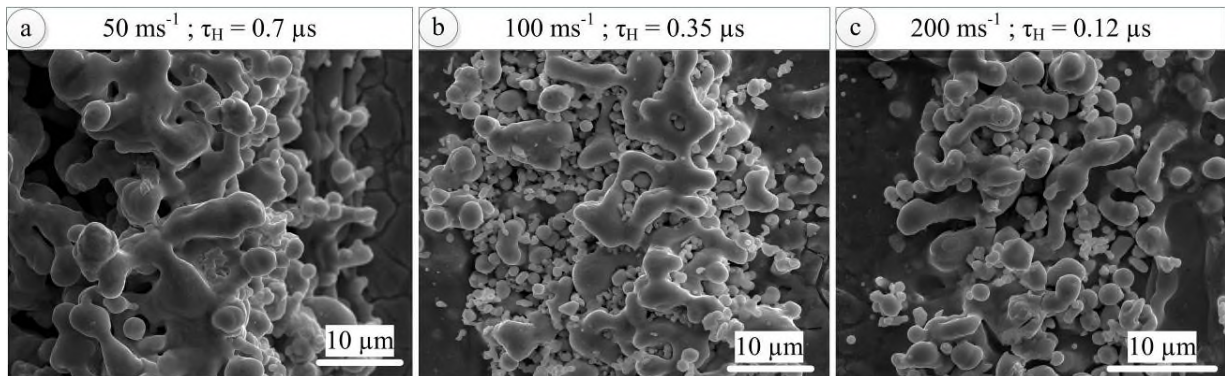


Fig. 16: Molten tracks of molybdenum powder at various high scan velocities and the respective short irradiation times. The applied cw-laser intensity was limited by the maximum power of the 400 W laser to $4 \cdot 10^7 \text{ Wcm}^{-2}$.

The decline of the fusion with the underlying sinter layer is apparent. At the highest scan velocities the resulting melt fusion occurs mainly in between the particles (Fig.16(c)), which is in the order of the calculated melt depth of about 1 μm . For noticeably better vertical fusion the irradiation times have to be 2-3 times longer than estimated for the respective sinter layer thickness. This corrected irradiation value approximates quite well the time that is required to obtain a critical melt depth in bulk material that equals the sinter layer thickness.

Furthermore, this relation corresponds to the necessary 2-3 - fold pulse overlap, and thus to the 2-3 - fold energy excess, that is required for the achievement of higher densities in laser micro sintering (Fig. 10).

Summary

In the last years, as a consequence of improvements in the powder coating technique, it became evident that highly resolved laser sintering with small powders does not necessarily imply abandonment of the high sinter densities that are achieved in laser melting with larger particles. With the available higher powder densities it had become possible to generate solid bodies with a line-wise strategy whereby remanent heat can be exploited. It was already anticipated that with tightly focused lasers that would supply sufficiently intense cw-radiation, rapid laser melting with high resolution would be feasible without the employment of q-switched pulses. Systematic experimental investigation has now delivered the proof that selective laser melting with resolutions comparable to the ones achieved in laser micro sintering can be executed with brilliant cw-laser-radiation.

The recently developed model of a crucial range concerning the combination of intensity, exposure time, and particle diameter for thorough fusion of metal powder particles was corroborated principally by experimental observations. However, already in the past, laser sintering praxis has revealed that comprehensive fusion of the discrete particles will not suffice, neither for overall fusion of a sinter layer nor for the fusion of a new sinter layer with the substrate or the previous layers. This “excessive” energy demand occurs also in laser melting with cw-radiation. This is another finding of the investigations.

Outlook

Rapid rate laser melting of bodies with highly resolved geometries can only be obtained with high scanning velocities. As the fusion of the powder still requires the merging of the melt entities originating from the powder particles, the hydrodynamic properties or the limited fluidity of the melt might become a limiting factor for a technology that relies on short irradiation times. Therefore, effects that influence the melt dynamic e.g. by rapid boiling or plasma pressure, which have been observed in laser micro sintering with q-switched pulses, could eventually become necessary.

It will be an interesting question if cw-lasers, with significantly higher power than and with comparable beam quality as the presently available ones, will yield the chance to supplement the technology of rapid scanning laser melting with the melt condensing effects that have been observed with q-switched pulses.

Appreciations

The presented experiments have been funded by ‘Bundesministerium für Bildung und Forschung’ of Germany in the course of the project ‘INNOPROFILE – Transfer’. The authors gratefully acknowledge the preparation of the probes and the assembling of the setup by Christin Schulze and Martin Erler.

References

- [1] C. Deckard, US patent 4,863,538. Filed: October 17th, 1986, published September 5th, 1989.
- [2] Shellabear, M., Nyrhilä, O.. Proceedings 4th LANE 2004, Sept. 22.-24. 2004, M. Geiger and A. Otto Eds., Meisenbach-Verlag, Erlangen, Germany, ISBN 3-87525-202-0, 393-404 (2004).
- [3] Exner, H., Regenfuss, P., Streek, A., German patent: DE102011014610, “Device for applying powder for additive fabrication process”, 03.05.2012
- [4] Streek, A. Ebert, R., Exner H.: “Innovative Fertigungstechnik, -verfahren und -planungsmethoden”, Technologiesymposium Oelsnitz, Germany 02.2014
- [5] Streek, A., „Beiträge zum Lasermikrosintern“, previously undisclosed Phd Thesis, University Dresden 2014.
- [6] Hügel, H., & Graf, T. (2009). Laser in der Fertigung. Laser in der Fertigung: Strahlquellen, Systeme, Fertigungsverfahren, ISBN 978-3-8351-0005-3. Vieweg+ Teubner Verlag| GWV Fachverlage GmbH, Wiesbaden, 2009, 1.
- [7] Streek, A., Regenfuss, P., Exner, H. „Fundamentals of Energy Conversion and Dissipation in Powder Layers during Laser Micro Sintering“, Proceedings LIM 2013, C. Emmelmann, M. Schmidt, M. Zäh and T. Graf Eds., Physics Procedia Elsevier B.V., Amsterdam, Netherlands.
- [8] Carslaw, H. (1959). S., Jaeger J., C., Conduction of Heat in Solids. Oxford Science Publications, ISBN 0, 19(853368), 3.